

https://dspace.org/

# Ligand design using the neutral oxygen donor to control metal ion size selectivity

**Bhavan, Rekha**

**2015-01-08**
http://hdl.handle.net/10539/16271

Downloaded from a DSpace repository. https://dspace.org/

# LIGAND DESIGN USING THE NEUTRAL OXYGEN DONOR TO CONTROL METAL ION SIZE SELECTIVITY

by

Rekha Bhavan

A Thesis presented in the

University of the Witwatersrand, Johannesburg

for the degree of Doctor of Philosophy

March 1989

# ABSTRACT

The synthesis of several novel macrocyclic ligands containing both oxygen and nitrogen donors, and containing in some cases also pendent donor groups bearing one or more oxygen donors is described. The formation constants of these ligands with a variety of metal ions are reported. Analysis of the formation constants shows that the presence of the neutral oxygen donor in ligands leads to stronger complexation of large metal ions relative to small metal ions, irrespective of whether the oxygen donor is part of the macrocyclic ring or not. However, addition of oxygen donors into the macrocyclic ring has a large effect on metal ion size selectivity. This is of interest in the design of chelating chemotherapeutic agents for the selective removal of toxic heavy metal ions such as $Pb^{2+}$, $Cd^{2+}$, and $Hg^{2+}$ from the body. The control of selectivity for the large $Pb^{2+}$ ion relative to the small $Zn^{2+}$ ion is examined. It is shown that the extra pair of oxygen donors in BHEE–18–ane $N_2O_4$ leads to an enhanced $Pb^{2+}/Zn^{2+}$ selectivity, as compared with the ligand BHE–18–ane $N_2O_4$. The ligand BHEE–18–ane $N_2O_4$ was found to have an acceptable $Pb^{2+}/Zn^{2+}$ selectivity of 7.2 log units. However, its affinity for $Pb^{2+}$ was rather too low to be used as a therapeutic agent for the treatment of $Pb^{2+}$ intoxication.

The crystal structure of three complexes of the above ligands are reported, [K(BHE–18–ane$N_2O_4$)]Cl (I), [K(BHEE–18–ane$N_2O_4$)]I (II), and [Ba(BHEE–18–ane$N_2O_4$)]$I_2$ (III). Compound I is sterically less crowded than compound II, and adopts the usual cis arrangement of the pendent donor groups, with all donor atoms involved in coordination. In contrast to compound I, the complex II appears to be sterically more crowded, with the pendent donor groups occupying the trans orientation, with at least two of the oxygen donors on the pendent groups being left uncoordinated. On the other hand, the $Ba^{2+}$ complex adopts the cis arrangement of

the pendent donor groups, with all donor atoms participating in coordination. The interaction of the extra oxygens on the $[Ba(BHEE-18-aneN_2O_4)]^{2+}$, explained why $Ba^{2+}$ produced an increase in complex stability as compared with the $DHP-18-aneN_2O_4$ complex.

The addition of extra bridging groups between nitrogen donors of macrocyclic ligands to give a nine–membered–ring–like structure, is expected to lead to more rigid macrocyclic ligands which should display genuine "hole–size–selectivity". As a starting point, the synthesis of a few open–chain analogues of these bridged ligands is described. The formation constants of these ligands with a variety of metal ions is reported. The results reinforce the ligand design principle observed previously, that five–membered chelate rings favour the complexation of large metal ions whereas six–membered chelate rings favour the complexation of small metal ions. This behaviour may not hold for the relatively inflexible macrocyclic bridged ligands.

## DECLARATION

I hereby declare that the work presented in this thesis was carried out exclusively by myself under the supervision of Prof. R.D. Hancock. This thesis has never been submitted for a degree in any other university.



R. Bhavan

To My Parents

## ACKNOWLEDGEMENTS

I would like to express my sincere appreciation to the following people for their contribution to the thesis:

My supervisor, Prof. R.D. Hancock, for his invaluable advice, guidance, encouragement and enthusiasm;

Peter Wade, for his help with the molecular mechanics calculations;

Dr. Sue Dobson, for her patient assistance with the X–ray crystallographic studies;

Dr. J.P. Michael for his advice on organic synthesis;

My family, friends and colleagues, for their support and assistance throughout the duration of this project;

The Council for Scientific and Industrial Research for their financial support.

# CONTENTS


| | | Page |
|---|---|---|
| List of Tables | | viii |
| List of Figures | | x |
| **CHAPTER** | | |
| 1. **INTRODUCTION** | | |
| 1.1 | General Introduction | 1 |
| 1.2 | The Types Of Donor Atoms | 4 |
| 1.3 | The Macrocyclic Effect | 10 |
| 1.4 | Macrocyclic Cavity Size | 15 |
| 1.5 | The Effect Of Chelate Ring Size | 25 |
| 1.6 | The Role Of The Oxygen Donor In Controlling Complex Stability | 35 |
| 1.7 | Rigid Macrocyclic Ligands | 42 |
| 1.8 | Aims Of This Study | 44 |
| 2. **EXPERIMENTAL** | | 46 |
| 2.1 | Instrumentation | 46 |
| 2.2 | Materials | 46 |
| 2.3 | Synthesis | 47 |
| 2.3.1 | DHP–15–ane $N_2O_3$ | 47 |
| 2.3.2 | 15–ane $N_3O_2$ | 47 |
| 2.3.3 | THP–15–ane $N_3O_2$ | 48 |
| 2.3.4 | 18–ane $N_4O_2$ | 49 |
| 2.3.5 | BHEE–18–ane $N_2O_4$ | 50 |
| 2.3.6 | BAE–9–ane $N_2O$ | 50 |
| 2.3.7 | BAP–9–ane $N_2O$ | 51 |
| 2.3.8 | BAE–10–ane $N_2O$ | 52 |
| 2.4 | Determination Of Stability Constants | 52 |
| 2.4.1 | Potentiometric Titrations | 52 |
| 2.4.2 | N.M.R. Spectroscopy | 53 |

Page

2.5 X–ray Crystallographic Studies 55
2.5.1 Preparation Of Crystals 55
2.5.2 Data Collection 56
2.5.3 Structure Determination 57

3. RESULTS AND DISCUSSION
3.1 The Contribution Of Cavity Size To Metal Ion Size–Selectivity 62
3.2 Oxygen Donors That Form Part Of The Macrocyclic Ring 67
3.3 Macrocycles With Pendent Arms Having Oxygen Donor Groups 76
3.4 The Structures Of The Complexes 90
3.5 The Complex Stability Of Alkali Cations With Macrocycles Containing Oxygen Donors 103
3.6 More Rigid Macrocyclic Ligands Containing Oxygen Donors 123

4. CONCLUSIONS 131

5. DIRECTIONS OF FUTURE RESEARCH 133

APPENDIX 1: Data For The Stability Constant Determination Using NMR Of The Alkali Nuclei 134

APPENDIX 2: Fractional Coordinates Of Structures Determined 142

APPENDIX 3: List Of Supplementary Material 150

REFERENCES 153

# LIST OF TABLES


| Table | | Page |
|---|---|---|
| 1. | Formation constants (log $K_1$) of complexes with some amines | 7 |
| 2. | Summary of the best–fit M–N distances obtained with different conformers of the tetraazamacrocycles | 18 |
| 3. | Formation constants (log $K_1$) data for 12–ane$N_4$ and 14–ane$N_4$ with a variety of metal ions | 21 |
| 4. | The difference in the total strain energies and enthalpy on complex formation on increasing the chelate ring size from five– to six–membered | 31 |
| 5. | Details of the crystallographic analysis | 58 |
| 6. | The formation constants of a variety of metal ions with the ligand DHP–15–ane $N_2O_3$, and those of some structurally similar ligands for comparison | 65 |
| 7. | Formation constant values of open–chain ligands and some mixed–donor macrocycles | 70 |
| 8. | Formation constants of a variety of metal ions with the ligands THP–15–ane $N_3O_2$; BHE–18–ane $N_2O_4$ and BHEE–18–ane $N_2O_4$ | 79 |
| 9. | Selected structural and binding parameters of the crystal structures determined | 92 |
| 10. | Total strain energies, $\Sigma U$, for the $K^+$ and $Ba^{2+}$ complexes of BHEE–18–ane–$N_2O_4$ | 100 |

| Table | | Page |
|---|---|---|
| 11. | Effective ionic radii (Å) of the $K^+$ and $Ba^{2+}$ cations as a function of the number of donors | 100 |
| 12. | Formation constants of some alkali metal ion complexes with various ligands studied in methanol at 23°C. | 109 |
| 13. | Total strain energy ($\Sigma U$) obtained for the alkali metal ion complexes with a variety of ligands | 121 |
| 14. | Protonation and Formation constants of ligands discussed in section 3.6 | 127 |

# LIST OF FIGURES


| Figure | | Page |
|---|---|---|
| 1.1.1 | Structures of chlorophyll and nonactin | 1 |
| 1.1.2 | Ethylenediaminetetraacetic acid | 3 |
| 1.1.3 | Structure of cryptand–2,2,2 | 4 |
| 1.2.1 | Structure of ligands given in Table 1 | 8 |
| 1.2.2 | Consequence of turning secondary nitrogens to tertiary nitrogens by replacing hydrogens on the donor atoms with methyl groups | 9 |
| 1.3.1 | The effect on complex stability in going from an open–chain ligand to a macrocyclic ligand | 10 |
| 1.3.2 | The open–chain ligand is able to accomodate more solvent molecules than the corresponding macrocyclic ligand | 11 |
| 1.3.3 | Effect on complex stability in going from an open–chain to a macrocyclic polyether | 14 |
| 1.4.1 | Structure of the tetraazamacrocycles and their hole–sizes as calculated by molecular mechanics for the metal ion lying in the plane of the nitrogen donors. Hole–size is the best–fit M–N bond length | 16 |
| 1.4.2 | Nomenclature for the configuration of coordinated tetraazamacrocycles | 17 |

| Figure | | Page |
|---|---|---|
| 1.4.3 | The trans–I and trans–III conformers of 12–aneN$_4$, showing diagrammatically that the trans–I conformer is much better able to accommodate large metal ions than is the trans–III | 19 |
| 1.4.4 | Total strain energy (U) versus r$^0$ curve for the trans–I forms of 12–aneN$_4$ and the trans–III form of 14–aneN$_4$ | 20 |
| 1.4.5 | Structures of some crown ethers | 22 |
| 1.4.6 | Cation binding by simple crown ethers | 23 |
| 1.5.1 | The effect of the chelate ring size | 26 |
| 1.5.2 | Effect of chelate ring size in both open–chain and macrocyclic ligands on the $Pb^{2+}$ over $Zn^{2+}$ selectivity | 28 |
| 1.5.3 | Change in complex stability, $\Delta$ log K, as a function of metal ion radius as the chelate ring is increased from five– to six–membered ring. The pair of ligands where the increase is occurring are EDTA and TMDTA | 29 |
| 1.5.4 | Stability of complexes of n–aneN$_4$ macrocycles relative to the stabilities of 12–aneN$_4$ complex as a function of n, the number of atoms in the macrocyclic ring of n–aneN$_4$ | 30 |
| 1.5.5 | Structures of the polyamines given in Table 4 | 30 |
| 1.5.6 | Strain energy versus [(M–N distances) and (N–M–N angles)] of a) a five membered chelate ring and b) a six membered chelate ring | 32 |

| Figure | | Page |
|---|---|---|
| 1.5.7 | The six–membered chelate ring | 33 |
| 1.5.8 | The five– and six–membered chelate bite size | 34 |
| 1.6.1 | Monensin–A antibiotic | 35 |
| 1.6.2 | Effect of addition of neutral oxygen donor groups to an existing ligand on the $Pb^{2+}/Zn^{2+}$ selectivity | 37 |
| 1.6.3 | Relationship between the change in complex stability, $\Delta$ log K, and the ionic radius of a variety of metal ions. The $\Delta$ log K values are for passing from EN to THPED and for EN going to cryptand–2,2,2 | 39 |
| 1.6.4 | The progressive increase in steric crowding around the small metal ion $Ni^{2+}$, leads to an increase in the Ni–O bond length | 41 |
| 1.7.1 | Structures of some rigid macrocyclic ligands | 43 |
| 2.5.3 | The structure and atomic numbering schemes of all the crystal structures determined | 60 |
| 3.1.1 | Structures of ligands discussed in section 3.1 | 63 |
| 3.1.2 | Effect of macrocyclic cavity size on the $Pb^{2+}/Zn^{2+}$ selectivity | 66 |
| 3.2.1 | The effect on the $Pb^{2+}$ over $Zn^{2+}$ selectivity as the number of oxygen donors are increased along the series of ligands | 71 |

| Figure | | Page |
|---|---|---|
| 3.2.2 | The change in complex stability, $\Delta$ log K, as a function of metal ion radius as one ethereal oxygen is added to DIEN to give 12–ane $N_3O$ or where two ethereal oxygen groups are added to DIEN to give 15–ane $N_3O_2$ | 72 |
| 3.2.3 | The change in complex stability, $\Delta$ log K, as a function of metal ion radius as two ethereal oxygens are added to TRIEN to give 18–ane $N_4O_2$ | 73 |
| 3.2.4 | The $Pb^{2+}$ stability constant of the 18–membered macrocycle showing the increase in stability on substitution of two nitrogens on each step | 74 |
| 3.3.1 | Effect of addition of hydroxypropyl groups to existing ligands on the $Pb^{2+}/Zn^{2+}$ selectivity | 76 |
| 3.3.2 | Structures of ligands discussed in section 3.3 and their selectivity of $Pb^{2+}$ over $Zn^{2+}$ | 78 |
| 3.3.3 | The change in complex stability $\Delta$ log K, as a function of metal ion radius, in going from DIEN to THP–15–ane $N_3O_2$ | 78 |
| 3.3.4 | The change in complex stability, $\Delta$ log K, as a function of metal ion radius, as $CH_2CH_2OH$ groups are added to 18–ane $N_2O_4$ to form BHE–18–ane $N_2O_4$ and when $CH_2CH_2OCH_2CH_2OH$ groups are added to 18–ane $N_2O_4$ to form BHEE–18–ane $N_2O_4$ | 81 |
| 3.3.5 | The $Pb^{2+}/Sr^{2+}$ selectivities for a series of ligands having a constant number of non–oxygen donor atoms | 84 |

| Figure | | Page |
|---|---|---|
| 3.3.6 | A possible way of achieving a high selectivity for $Pb^{2+}$ over $Zn^{2+}$ is by adding oxygen–donor bearing groups to existing ligands | 85 |
| 3.3.7 | The change in complex stability relative to EN as hydroxy–ethyl groups are added to EN to give,successively, HEEN, DHEEN, and THEEN | 87 |
| 3.3.8 | Ideal geometries for the five– and six–membered chelate rings | 89 |
| 3.4.1 | Skeletal diagram of the potassium complex of BHE–18–ane $N_2O_4$ | 93 |
| 3.4.2 | Stereo view of the major conformer of $[K(BHEE–18–ane\ N_2O_4)]^+$ | 93 |
| 3.4.3 | Skeletal diagram illustrating the donor atoms of a) the major conformer and b) the minor conformer of $[K(BHEE–18–ane\ N_2O_4)]I$ | 95 |
| 3.4.4 | The unit packing diagram of $[Ba(BHEE–18–ane\ N_2O_4)]I_2 \cdot 3H_2O$ | 98 |
| 3.4.5 | Skeletal diagram illustrating the donor atoms of $[Ba(BHEE–18–ane\ N_2O_4)]I_2 \cdot 3H_2O$ | 98 |
| 3.4.6 | Relationship between change in complex stability, $\Delta$ log K, which occurs when changing a five–membered chelate ring to a six–membered chelate ring, and the ionic radius of the metal ion | 102 |
| 3.5.1a | $^{23}Na$ chemical shifts as a function of the ligand/$Na^+$ mole ratio in methanol | 106 |

| Figure | | Page |
|---|---|---|
| 3.5.1b | $^{87}Rb$ chemical shifts as a function of the ligand/$Rb^+$ mole ratio in methanol | 107 |
| 3.5.1c | $^{133}Cs$ chemical shifts as a function of the ligand/$Cs^+$ mole ratio in methanol | 108 |
| 3.5.2 | $^{23}Na$ NMR spectra of $Na^+$–15–ane $N_2O_3$ and $Na^+$–DHP–15–ane $N_2O_3$ in methanol at 23°C | 110 |
| 3.5.3 | $^{23}Na$ NMR spectra of $Na^+$–15–ane $N_3O_2$ and $Na^+$–THP–15–ane $N_3O_2$ in methanol at 23°C | 111 |
| 3.5.4 | $^{87}Rb$ NMR spectra of $Rb^+$–15–ane $N_2O_3$ and $Rb^+$–DHP–15–ane $N_2O_3$ in methanol at 23°C | 112 |
| 3.5.5 | $^{87}Rb$ NMR spectra of $Rb^+$–15–ane $N_3O_2$ and $Rb^+$–THP–15–$N_3O_2$ in methanol at 23°C | 113 |
| 3.5.6 | $^{133}Cs$ NMR spectra of $^{133}Cs$–15–ane $N_2O_3$ and $^{133}Cs$–DHP–15–ane $N_2O_3$ in methanol at 23°C | 114 |
| 3.5.7 | $^{133}Cs$ NMR spectra of $^{133}Cs$–15–ane $N_3O_2$ and $^{133}Cs$–THP–15–ane $N_3O_2$ in methanol at 23°C | 115 |
| 3.5.8 | Effect of N–substitution on complex stability of alkali cation complexes | 116 |
| 3.5.9 | Effect of addition of oxygen donors on the complex stability of alkali metal ions | 118 |
| 3.5.10 | Formation constants, log $K_1$, in methanol for a variety of ligands complexing with the alkali metal ions, as a function of crystal radius | 120 |

| Figure | | Page |
|---|---|---|
| 3.5.11 | The components of the energies contributing to the final stability order observed for 18–crown–6 complexes with the alkali metal ions, as a function of radius | 120 |
| 3.5.12 | The change in total strain energy versus ionic radius for the pair of ligands indicated | 122 |
| 3.6.1 | Structures of some rigid macrocycles and their open–chain analogues discussed in this section | 126 |
| 3.6.2a | Change in complex stability, $\Delta$ log K, as a function of metal ion radius, in going from BAE–9–ane $N_2O$ to BAE–10–ane $N_2O$ | 129 |
| 3.6.2b | Change in complex stability, $\Delta$ log K, as a function of metal ion radius, in going from BAP–9–ane $N_2O$ to BAE–9–ane $N_2O$ | 129 |

# CHAPTER 1

# INTRODUCTION

## 1.1 GENERAL INTRODUCTION

The discovery of the template reactions by Curtis (1) and the crown ethers by Pedersen (2) became the starting point for the synthesis of a large number of macrocycles.

Previously most research on synthetic macrocylic ligands was focussed on complexes of porphyrins, corrins and phthalocyanins because of their relation to the naturally occurring macrocylic complexes such as heme, cytochromes and chlorophyll (3b) (Fig. 1.1.1). The coordination chemistry of these naturally occurring macrocycles was poorly understood and synthetic macrocycles became an important tool in understanding the function of the metal ion in such systems.

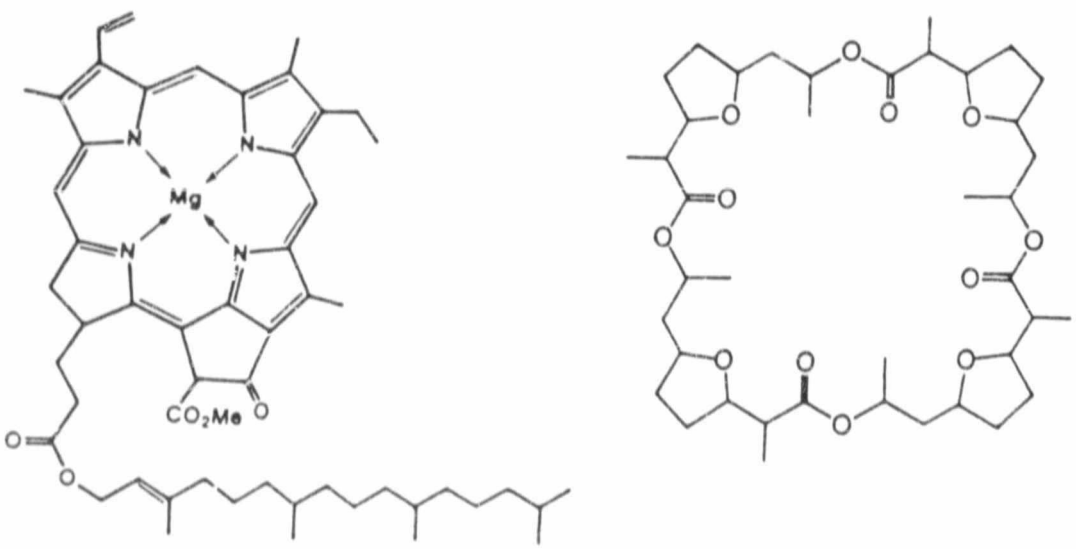


a b

Fig. 1.1.1 Structures of (a) chlorophyll and (b) nonactin

Complexes of tetraazamacrocycles have been extensively studied due to the occurrence of these systems in biological structures such as heme and vitamin $B_{12}$ (3a) and the importance of the oxygen donor macrocycles in the coordination chemistry of alkali– and alkaline earth–metal ions exhibit potential significance in biological systems particularly with respect to ion transport and antibiotics (3a).

To date, a large number and variety of macrocycles have appeared in the literature (4,25) and the possible application in both analytical and medical fields is well documented (5,6). Nevertheless, these macrocycles have certain limitations and the improvement of the metal ion selectivity of these ligands is still required. There is thus a need for the synthesis of ligands which have specific binding properties. To achieve this, various ligand design features need to be considered, such as factors which affect the stability of metal complexes and geometric preferences imposed by the ligand and metal ion. A good design should produce a ligand that can be easily synthesized incurring as little cost as possible.

Our main interest is in the development of macrocyclic ligands as therapeutic agents for the treatment of metal intoxication. Particularly important is the metal ion lead, which has become a major environmental pollutant and whose toxicity represents one of the most serious problems.

While other sources of lead include paints, putty, soil, dust and plumbing, practically all the lead found in the environment (200 000 tons per annum) (7,8) comes from exhaust fumes. Consequently, almost everyone living in industrialized areas is at a risk of being subjected to high levels of lead contamination.

The toxic effects of lead are widespread but the most sensitive area is the hematopoietic system where it causes a decrease in the survival of red blood cells

and inhibits heme synthesis. Other effects which include sterility, abortion and stillbirths have also been reported (9). Another serious effect of lead toxicity is that it causes damage to the central nervous system of growing children, thus causing damage to brain function and development (10).

The current antidote used for lead poisoning is EDTA (11) (Fig. 1.1.2) but this has major limitations. Being an open chain ligand, EDTA is able to accommodate a variety of metal ions. It complexes strongly with metal ions such as zinc(II) and calcium(II). These metal ions are essential for normal physiological processes that occur in the body. By employing EDTA, large amounts of zinc and calcium are removed from the body during treatment. To overcome the depletion of calcium and zinc the drug is administered as a calcium complex and the patient is periodically supplemented with zinc.

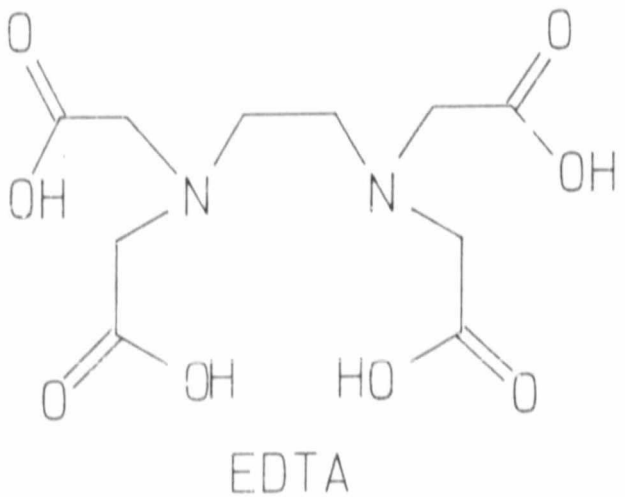


Fig. 1.1.2 Structure of ethylenediaminetetraacetic acid (EDTA)

An improvement over EDTA, as suggested by Lehn (12) would be cryptand–2,2,2 (Fig. 1.1.3) since it is a more lead–selective ligand, with a lead over zinc selectivity of 9 log units compared to the 1.44 log units of EDTA. The major setback with

cryptand–2,2,2 is that complex formation occurs very slowly and it is also expensive, a feature which makes the use of EDTA more advantageous.

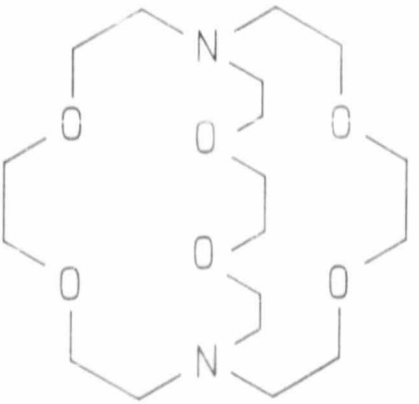


Fig. 1.1.3 Structure of cryptand–2,2,2.

In this work the aim is to design and synthesize macrocyclic ligands which will show an enhanced lead over zinc selectivity. An important feature to consider when designing such ligands is that the toxic metals such as lead, cadmium and mercury form large metal ions whereas the biologically essential metal ions such as zinc, copper and iron form small metal ions. By exploiting this metal ion size difference, ligands which are selective for large metal ions can be designed and so alter ligand selectivity for large over small metal ions.

In order to establish certain ligand design features it is necessary to examine the factors which control the stability of metal complexes.

## 1.2 THE TYPES OF DONOR ATOMS

The choice of donor atom has been discussed on the basis of Pearson's (13) concept of "hard" and "soft" acids and bases (HSAB). Hard metal ions such as the alkali– and alkaline earth–metal ions prefer hard donor atoms such as O, S and F⁻

whereas the soft metal ions such as $Cu^{+}$, $Hg^{2+}$ and $Ag^{+}$ prefer the soft donor atoms such as $I^{-}$ and $CN^{-}$. The major setback of this classification is that some of the transition metal ions, namely, $Cu^{2+}$, $Zn^{2+}$, $Co^{2+}$, $Ni^{2+}$ and $Pb^{2+}$ are borderline cases, in that these cannot be classified as either hard or soft metal ions. Therefore, the choice of donor atoms for these metal ions cannot be easily predicted. However, the HSAB classification does provide a useful starting point for the selection of donor atoms.

The discussion will be limited to saturated nitrogen and neutral oxygen donor atoms, since this work relates to mixed nitrogen and oxygen donor macrocycles.

### 1.2.1 Relative Strength of the Donor Atoms

Gas phase studies by Taft et al. (14) indicate that the strength of the oxygen donor increases in the gas phase in the order

$$H_2O<ROH<R_2O$$

and that of the nitrogen donor in the gas phase increases in the order

$$NH_3<RNH_2<R_2NH<R_3N$$

where R = methyl group.

As hydrogens are replaced by methyl groups the intrinsic basicity increases, so ROH and $R_2O$ are more basic than $H_2O$, and $R_3N$, $R_2NH$ more basic than $NH_3$. Since it is the basicity that governs the strength of the donor atoms, the implication is that ROH, $R_2O$ are stronger donors than $H_2O$ and $R_3N$, $R_2NH$ stronger donors than $NH_3$.

Brauman et al. (15,16) have reported that the basicities of amines in the gas phase would increase with increase in N–methylation and found that with an increase in $\alpha$–C methylation the order was

$$CH_3NH_2<RCH_2NH_2<R_2CHNH_2<R_3CNH_2$$

where R = methyl group. By exte. ding the gas phase basicity studies to other amines, Brauman and Blair (17) found the relative basicities to be

$$Et_3N > Et_2NH > EtNH_2 > NH_3$$

The increase in basicity of the amines was attributed to polarizability and inductive effects.

The polarizabiliy effect is explained in terms of the delocalization of charges on the molecular ion formed in the gas phase. The more charge that is delocalized over the molecular ion, the more it is stabilized. Larger molecules can delocalize charges more effectively than smaller molecules, because they consist of more atoms and bonds. Thus, larger molecules will have greater proton affinities. Hence, as more methyl groups are substituted on the nitrogen, the basicity of the amine increases.

The inductive effect is explained in terms of the electron–donating ability of the methyl groups. The methyl groups being electron donating cause the nitrogen donor to become more electron rich, thus increasing its affinity for the proton and hence the basicity of the amine.

With an increase in the basicity of the donor atom, an increase in complex stability is expected. As a result, ligands with tertiary amines should form more stable complexes than those formed with secondary amines which in turn should form more stable complexes than complexes formed with primary amines. This increase in complex stability is not observed, as the data in Table 1 suggests. The nitrogen donors of the ligand TM–12–ane$N_4$ are all tertiary but the metal complexes formed by this ligand are destabilized relative to 12–ane$N_4$ which has secondary nitrogen donors. Similar behaviour is observed with the pair of ligands EN and TMEN. The stability of the metal complexes is thought to be governed by the delicate balance between steric and inductive effects (18). The destabilization

produced by the above ligands is thus attributed to the large steric strain produced by the methyl substituents. A more serious effect of methyl substitution on complex stability is observed in TM–14–aneN$_4$. For Cu(II) the log K$_1$ value drops from 27.2 with 14–aneN$_4$ to a value of 18.2 with TM–14–aneN$_4$ and for Ni(II) the decrease is from 22.2 with 14–aneN$_4$ to 8.6 for TM–14–aneN$_4$. Thus, the greater basicity of the nitrogen donors in TM–14–aneN$_4$ does not necessarily lead to an increase in complex stability. The decrease in stability is because the methyl substituents produce a dramatic increase in steric strain (Fig. 1.2.2). Molecular mechanics calculations (83) show that the total strain energy, $\Sigma U$, increase from 11.3 kcal mol$^{-1}$ in [Ni(14–aneN$_4$)]$^{2+}$ to 35 kcal mol$^{-1}$ in [Ni(TM–14–aneN$_4$)]$^{2+}$.

Table 1. Formation Constants (Log K$_1$) of Complexes With Some Amines

| Ligand | $Cu^{2+}$ | $Ni^{2+}$ | $Zn^{2+}$ | $Cd^{2+}$ | $Pb^{2+}$ |
|---|---|---|---|---|---|
| EN[a] | 10.71 | | 5.87 | 5.62 | 5.04 |
| TMEN[a] | 7.38 | | 3.62 | 3.87 | |
| 12–aneN$_4$[b] | 23.29 | 16.4 | 16.2 | 14.3 | 15.9 |
| TM–12–aneN$_4$[c] | 18.37 | | 14.04 | 13.06 | 13.91 |
| 14–aneN$_4$[b] | 27.2 | 22.2 | 15.5 | 11.23 | 10.83 |
| TM–14–aneN$_4$[d] | 18.3 | 8.6 | 10.4 | 9.0 | |

[a] Ref. 20 [b] Ref. 102 [c] Ref. 21 [d] Ref. 101

Structures of the above ligands are given in Fig. 1.2.1.

The log K$_1$ values for TMEN are reported at ionic strength of 0.5




EN TMEN

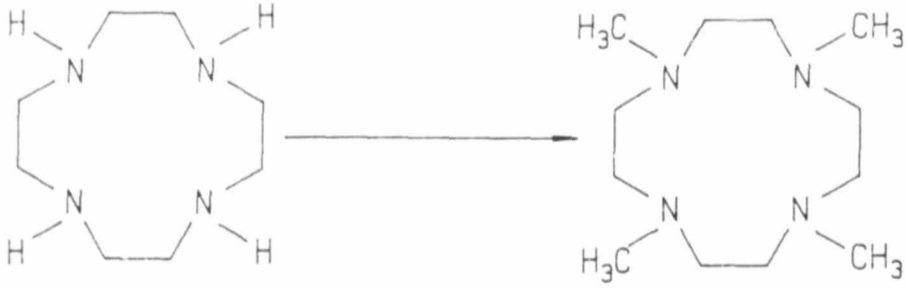


12-aneN4 TM-12-aneN4

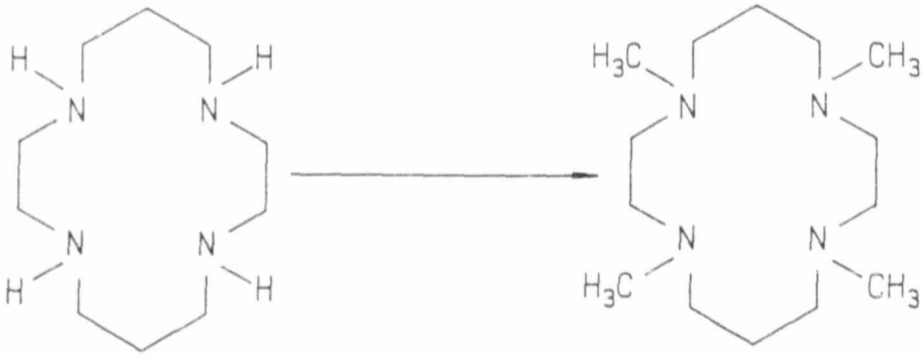


14-aneN4 TM-14-aneN4

Addition of methyl groups to the macrocycle turns secondary nitrogens into tertiary nitrogens.

The result: destabilization of complex stability.

Fig. 1.2.1 Structures of the ligands given in Table 1.

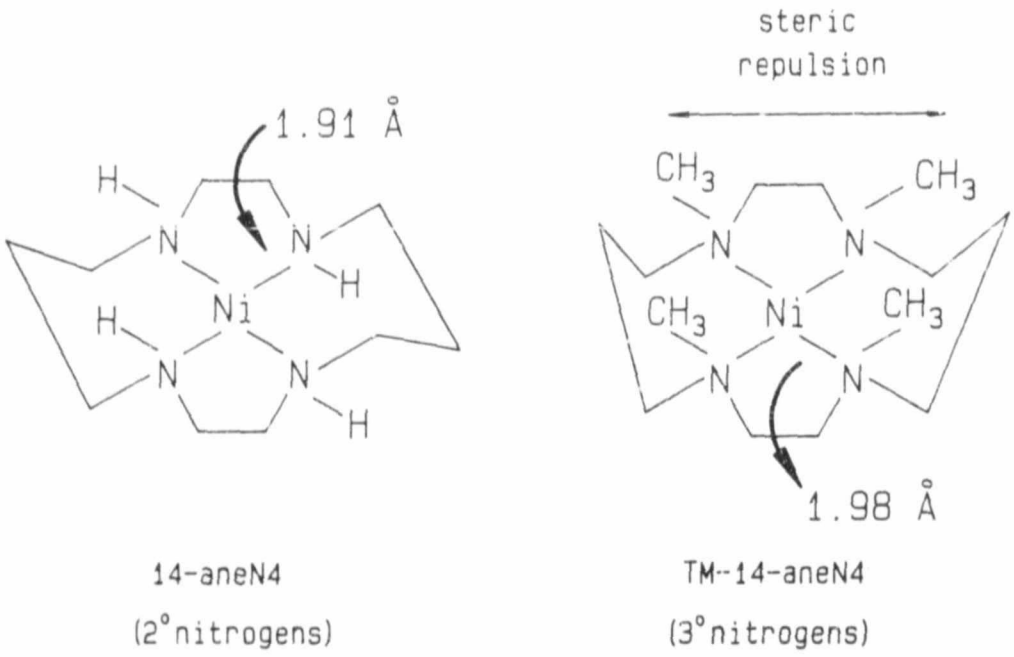


Fig. 1.2.2 Consequence of turning secondary nitrogens to tertiary nitrogens by replacing hydrogens on the donor atoms with methyl groups.

The drop in complex stability is accompanied by a drop in ligand field strength from a value of $Dq_{xy}$ = 2043cm$^{-1}$ in $[Ni(14\text{–}aneN_4)]^{2+}$ to 1782cm$^{-1}$ in $[Ni(TM\text{–}14\text{–}aneN_4)]^{2+}$ (19). This decrease in ligand field indicates a decrease in the overlap in the M–N bond and is observed when M–L bonds are stretched in response to steric strain. Molecular mechanics calculations (83) predict the M–N bond lengths to be 1.91Å in $[Ni(14\text{–}aneN_4)]^{2+}$ and 1.98Å in $[Ni(TM\text{–}14\text{–}aneN_4)]^{2+}$. The calculations agree well with the observed M–N bond lengths found in the crystal structure of $[Ni(TM\text{–}14\text{–}aneN_4)]^{2+}$ (26). Th. stretching of the Ni–N bonds in $[Ni(TM\text{–}14\text{–}aneN_4)]^{2+}$ is due to Van de Waals repulsion between the N–methyl groups.

The addition of alcoholic (ROH) or ethereal ($R_2O$) oxygen atoms to primary amines should enhance the stability of metal complexes. A large amount of data

suggest (32, 38, 60–62, 64) that when neutral oxygen donors are added to either a primary or a secondary amine the complexation of large metal ions is favoured over the small metal ions, an important feature to consider when designing ligands for the improvement of metal–ion size–selectivity. This feature forms a major theme of this work and is discussed further in section 1.6.

## 1.3 THE MACROCYCLIC EFFECT

The macrocyclic effect was first demonstrated by Cabbiness and Margenum (40) who observed that macrocyclic ligands formed more stable complexes with metal ions than open chain ligands of similar structure (Fig. 1.3.1). The increase in stability of the macrocyclic complex was in the order of $10^4$. Subsequently, the enhanced stability of other macrocyclic complexes have been well established.

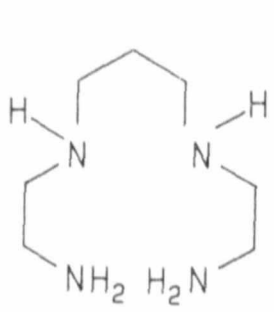

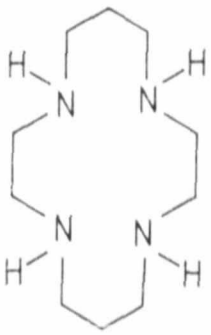

| | Open-Chain | Macrocycle |
|---|---|---|
| Log $K_1$: $Pb^{2+}$ | 7.8 | 10.8 |
| Log $K_1$: $Cu^{2+}$ | 23.2 | 26.5 |

Increase in complex stability in the order of $10^4$

Fig. 1.3.1 The effect on complex stability in going from an open–chain ligand to a macrocyclic ligand.

The macrocyclic effect is the change in Gibbs free energy (41) for the reaction

$$ML^{n+1} + Lm \longrightarrow MLm^{n+1} + L$$

noncyclic macrocyclic macrocyclic noncyclic

Since both enthalpy and entropy terms contribute to the Gibbs free energy, it was necessary to study these components separately. The first attempts to separate these components led to opposing conclusions.

Hinz and Margerum (42) suggested that ligand solvation enthalpy was largely responsible for the macrocyclic effect. When comparing the formation constants of Ni(cyclam)$^{2+}$ and Ni(2,3,2–tet)$^{2+}$, the authors found a difference of 6.8 log units in going from the linear amine to the cyclic amine. The greater stability of the cyclic complex was due to a favourable enthalpy change (–14 kcal.mol$^{-1}$). It was proposed (42) that since the cyclic ligand was more compact than the noncyclic ligand, it would be less solvated since it would not be able to accommodate as many H–bonded water molecules with the nitrogen donors and consequently would have a more negative enthalpy change (Fig. 1.3.2).

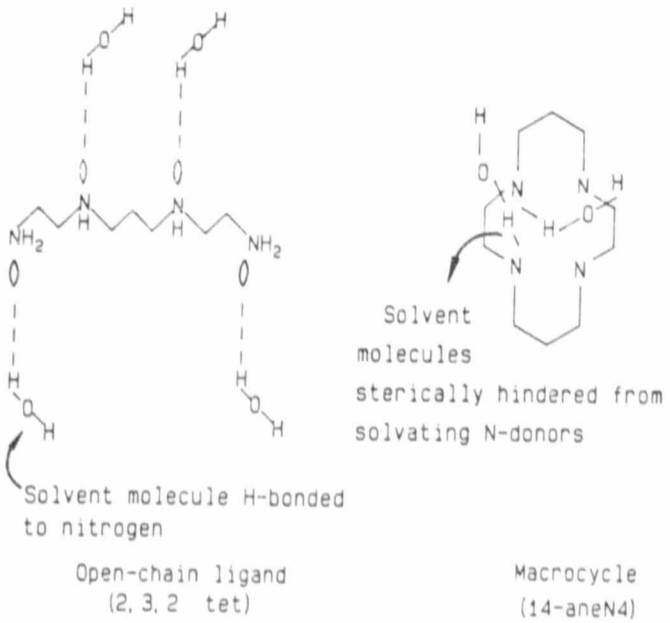


Fig. 1.3.2 The open–chain ligand is able to accommodate more solvent molecules than the corresponding macrocyclic ligand.

The open chain ligand would have a higher configurational entropy than the corresponding cyclic ligand so that on complex formation there would be a greater loss in configurational entropy for the open–chain ligand compared to the macrocyclic ligand. Hinz and Margerum (42) concluded that while the configurational entropy contributes to the enhancement of complex stability it is outweighed by the ligand desolvation enthalpy in hydrogen bonding solvents.

However, Paoletti et al. (43) and Kodama and Kimura (44) proposed that the macrocyclic effect resulted from favourable entropy factors. Paoletti et al. (43) reported enthalpies of complexes of both $Cu^{2+}$ and $Zn^{2+}$ with the macrocyclic ligands 12–ane$N_4$, 14–ane$N_4$ and 15–ane$N_4$. The conclusion was that there will always be a favourable entropy contribution to the macrocyclic effect. This arises because macrocycles are "preorientated", as suggested by Fabbrizzi et al. (41). Before coordination the macrocyclic ligand has donor groups in approximately the correct positions and therefore on complex formation does not lead to unfavourable strain energies. In contrast, its open chain analogues have in solution a lower strain energy when in the uncoordinated form than when coordinated (41). This implies that the macrocycle would not lose configuration entropy to the same extent as the open–chain ligand on complex formation (43). The magnitude of the macrocyclic enthalpy present was dependent on how best the metal–ion size matched the size of the aperture in the macrocyclic ligand (43).

Kodama and Kimura (45) have reported thermodynamic studies of complex formation of various metal ions with tri– and penta–amines and found that ligand cyclization had little effect on the change in enthalpy and more serious effect on the change in entropy on complex formation with these macrocycles. There was some correlation between the macrocyclic effect and the ratio of the size of the metal ion to the size of the macrocyclic cavity.

McDougall et al. (46) examined the crystal structure of the protonated cyclam and found it to be of an almost identical conformation to the structure of the $Ni^{2+}$ complex. Since the macrocycle was already in the conformation required for complex formation the increase in the strain energy on complex formation should be small. This was in contrast to open–chain polyamines where there was a large increase in strain energy upon complex formation. The authors suggested that the macrocyclic effect could be partly due to the ligand being "prestrained". To investigate this further Hancock et al. (47) carried out molecular mechanics calculations on the $Ni^{2+}$ complexes of polyamines. The main contributions to the macrocyclic enthalpy were 1) more secondary nitrogen–donors unaccompanied by the usual increase in strain energy normally associated with changing a primary to a secondary nitrogen and 2) the high value of strain energy for the free ligand is caused by dipole–dipole repulsion in the gas phase, which may be somewhat modified by steric hinderance to solvation in aqueous solution.

The presence of the macrocyclic effect in cyclic polyethers was first demonstrated by Frensdorff (48) who noted that there was an increase of $10^3$–$10^4$ orders of magnitude between the stabilities of complexes formed with 18–crown–6 and its open chain analogue, pentaglyme (Fig. 1.3.3).

The thermodynamic data of complex formation by these ligands revealed no reproducible trends in changes in the enthalpy or entropy among the cations studied which could explain the macrocyclic effect (49).

The postulate of Hinz and Margerum (42) that the difference in solvation between cyclic and open chain ligands is responsible for the macrocyclic effect, suggests that the stabilities of complexes of 18–crown–6 and pentaglyme determined in solvents of different solvating strength and dielectric constant should

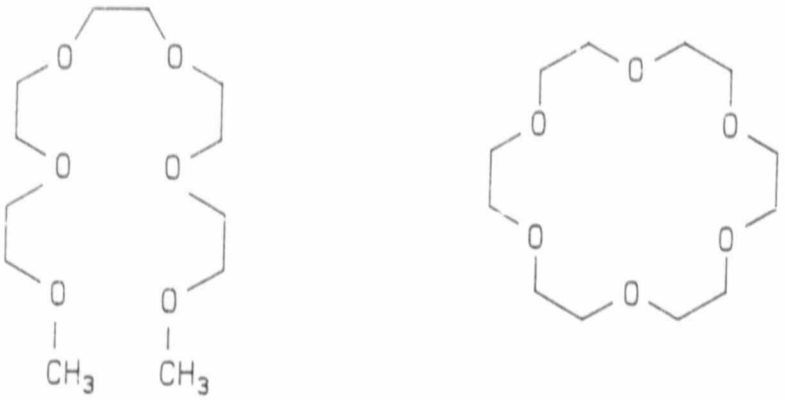


Fig. 1.3.3 Effect on complex stability in going from an open–chain to a macrocyclic polyether.

produce different results. Izatt et al. (50) measured the stabilities of the polyether–cation complexes in solvents of different ionic strengths. If solvation plays an important role in the stability of these complexes then the macrocyclic effect should increase in solvents with a larger dielectric constant. The results obtained (50) were contrary to this. Thus, it was concluded that the contribution of solvation to the macrocyclic effect of polyethers was not important.

Kollman et al. (31) have used molecular mechanics calculations to analyse the macrocyclic effect observed in crown–ether complexes. The formation energies calculated for the complexes indicated that there was an enthalpic contribution to the macrocyclic effect The low–energy conformation of free pentaglyme has to

undergo more energetically unfavourable rearrangement for complexation than the macrocycle, implying that the macrocycle is "preorientated" as observed for other systems (41,46). The macrocyclic effect was expected to decrease with increase in the dielectric constant of the medium (31) because of stabilization of electrostatic repulsions in such solvents. This explains the results obtained by Izatt et al. (50).

For mixed–donor macrocycles containing S,N, and O donors, Arnaud–Neu et al. (103) concluded that both enthalpy and entropy contributed to the macrocyclic effect.

Other properties that are typical of macrocyclic complexes, in addition to the thermodynamic stability, include: a) the ability of macrocycles to stabilize unusual oxidation states of metal ions (66); b) the kinetic inertness both towards complex formation and decomposition (51) and c) strong M–N interactions which are reflected in the high ligand field parameter, 10Dq (67).

## 1.4 MACROCYCLIC CAVITY SIZE

The structural parameter that is characteristic of macrocyclic ligands is the cavity in the centre of the ligand. An important idea that emerges from this is that the ligand can display selectivity towards metal ions on the basis of their size. One would thus expect an increase in stability for metal ions that fit best in the macrocyclic cavity so that large metal ions prefer large cavities and small metal ions prefer small cavities. Much research has therefore been focussed on ring–size–selectivity in macrocyclic ligands.

Using molecular mechanics calculations Busch et al. (22) have calculated ring sizes of a series of saturated tetraazamacrocycles (Fig. 1.4.1) for the metal ion

constrained in the plane of the nitrogen donors of the ligand. The ideal ring size corresponded to the M–N bond length which produced the minimum strain energy, which for 12–ane$N_4$ is 1.82Å; 13–ane$N_4$, 1.92Å; 14–ane$N_4$, 2.07Å; 15–ane$N_4$, 2.22Å and 16–ane$N_4$, 2.38Å. This work was later supported by Hancock et al. (23). Maximum stability was expected for metal complexes with the macrocycle in the above series which best fitted the bond length requirements of the metal ion. When this work was carried out stability constant data was not yet available to support their findings.

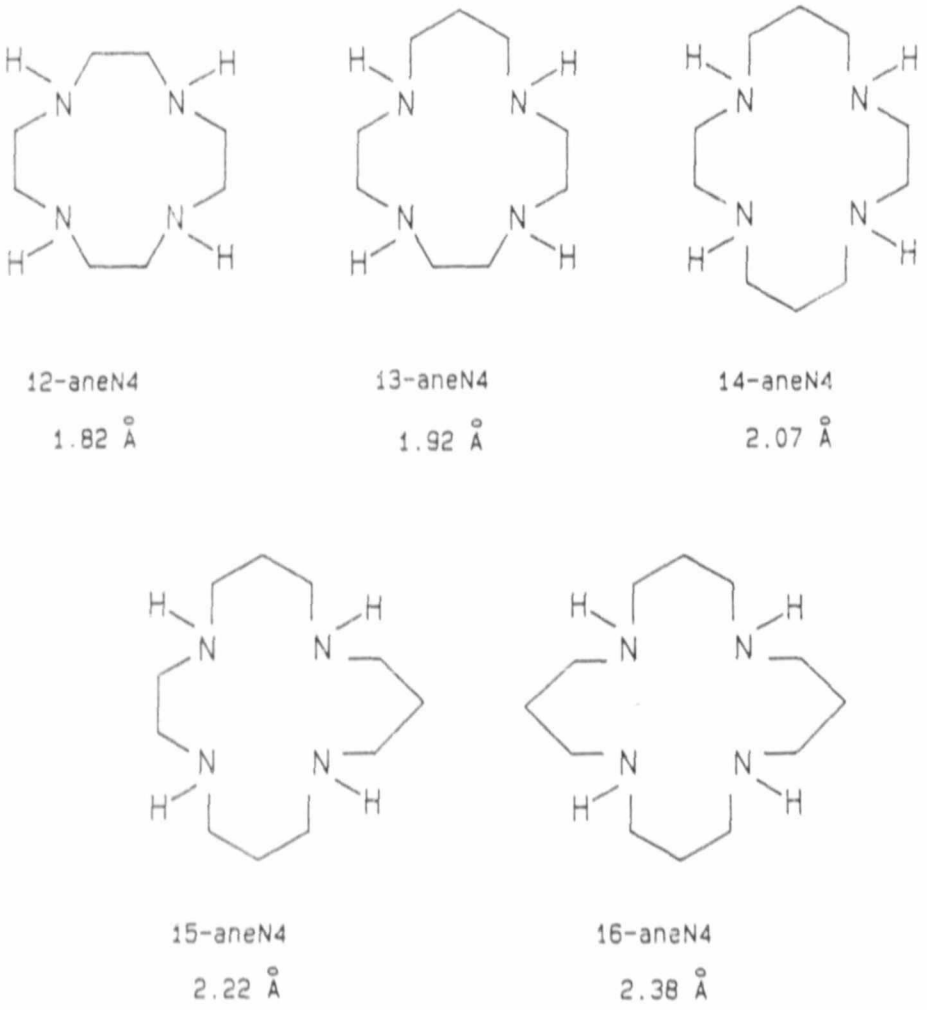


Fig. 1.4.1 Structure of the tetraazamacrocycles and their hole–sizes as calculated by Molecular Mechanics for the metal ion lying in the plane of the nitrogen donors. Hole–size is the best fit M–N bond length.

The above calculations were performed on a single conformer of each macrocycle (22,23). Hancock et al. (24) later reported molecular mechanics calculations on different conformers (Fig. 1.4.2) of these macrocycles.

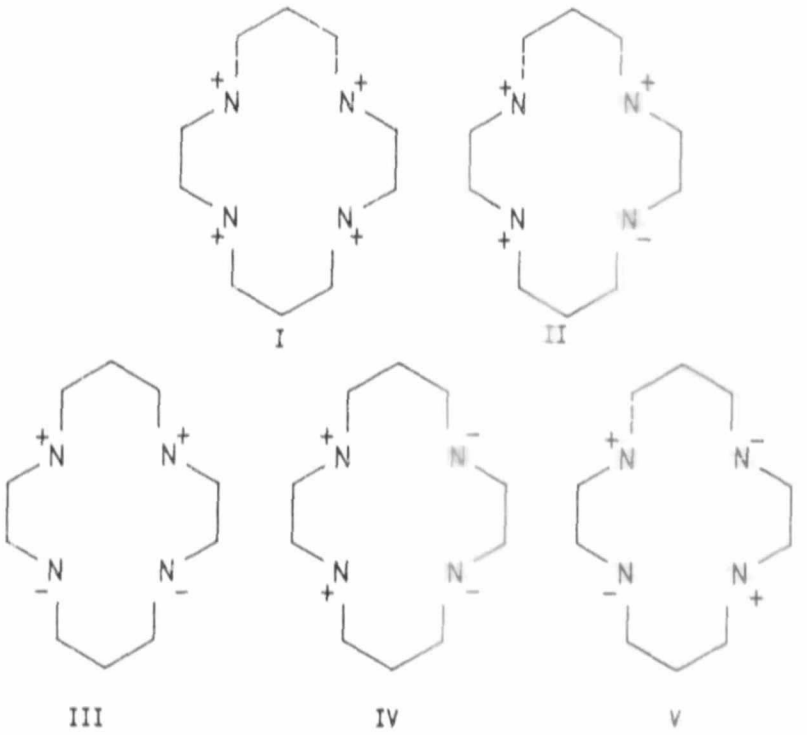


Fig. 1.4.2. Nomenclature for the configuration of coordinated tetraazamacrocycles. The (+) indicates the H of the NH group is above the plane of the flattened macrocycle, while the (−) indicates that it is below. The macrocycle shown is 14–ane$N_4$. Reproduced with permission from ref. 24.

These calculations revealed that in the case of 12–ane$N_4$ the trans I conformer is the most stable as indicated by the lowest strain energy whereas the trans III conformer is the least stable indicated by the higher strain energy. With 13–ane$N_4$ the trans III conformer had the lowest strain energy while the trans III conformer of 14–ane$N_4$ gave the lowest strain energy between M–N distances of 1.9Å and 2.29Å. The best–fit M–N distances obtained are summarized in Table 2. It is

evident from the data given in Table 2 that the trans I isomer of the smaller macrocycle 12–aneN$_4$, shows a preference for larger metal ions. This is contrary to the previous theory on "hole–size" selectivity.

Table 2. Summary of the Best–Fit M–N distances obtained with different conformers of the tetraazamacrocycles

| Ligand | Square–Planar Geometry | | Square–Pyramidal Geometry | | Octahedral Geometry | |
|---|---|---|---|---|---|---|
| | Favoured Conformer | best–fit size | Favoured Conformer | best–fit size | Favoured Conformer | best–fit size |
| 12–aneN$_4$ | trans–I | 2.11 | trans–I | 2.11 | trans–III | 1.81 |
| 13–aneN$_4$ | trans–III planar | 1.92 | trans–I | 2.03 | trans–III planar | 1.92 |
| | | | trans–III out of plane | 1.98 | | |
| 14–aneN$_4$ | trans–III planar | 2.05 | trans–III | 2.05 | trans–III planar | 2.05 |
| | | | trans–I | 2.00 | cis–v folded | 2.15 |

Data from ref. 24.

If the metal ions are constrained to lie in the plane of the macrocycle, then large metal ions would be expected to complex most strongly with larger macrocycles, while smaller metal ions would be strongly complexed by smaller macrocycles.

However, calculations by Hancock et al. (24) reveal that when metal ions are too large for the cavities then in the trans I conformer, the metal ion can coordinate out of the plane of the donor atoms (Fig. 1.4.3).

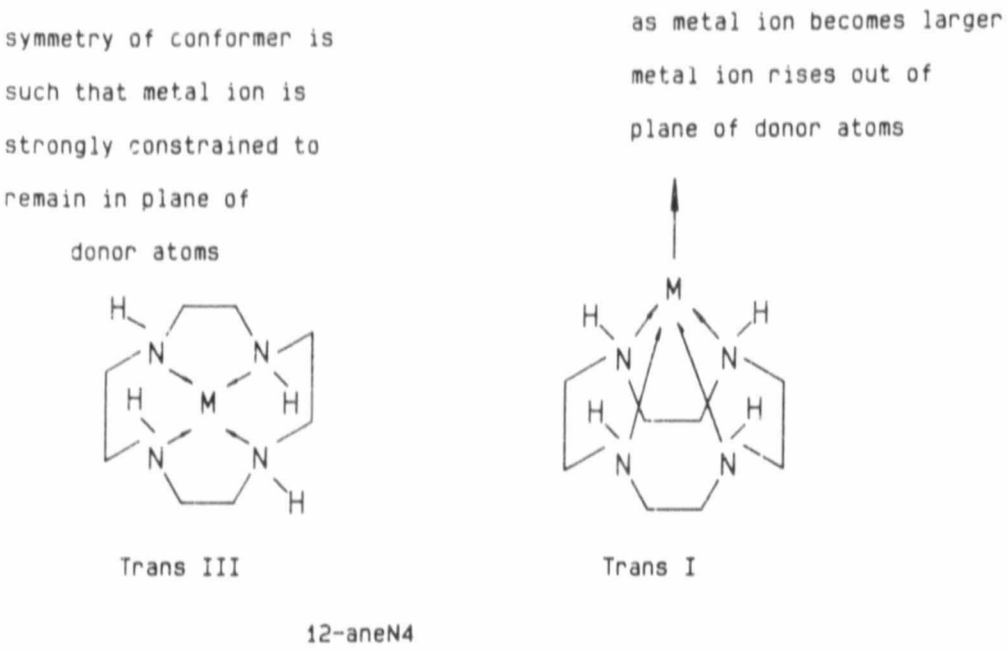


Fig. 1.4.3 The trans–I and trans–III conformers of 12–ane$N_4$, showing diagrammatically that the trans–I conformer is much better able to accommodate large metal ions than is the trans–III. Redrawn after ref. 100.

An important consequence of these calculations is that tetraazamacrocycles can easily change conformation to accommodate large metal ions and the coordination of metal ions is not restricted to being in the plane of the donor atoms. Therefore, the cavity size does not play a large role in controlling metal ion size–selectivity. It is rather the relative stabilities of the different conformers that governs this metal ion size–selectivity. Since the trans I conformer is more flexible it will be able to accommodate a full range of .netal ions whereas the more rigid trans III conformer would not coordinate well to large metal ions. This is shown diagramatically in Fig. 1.4.4. The total strain energy is plotted as a funtion of the metal ion size. The sharper the curve, the sharper the metal–ion size–selectivity.

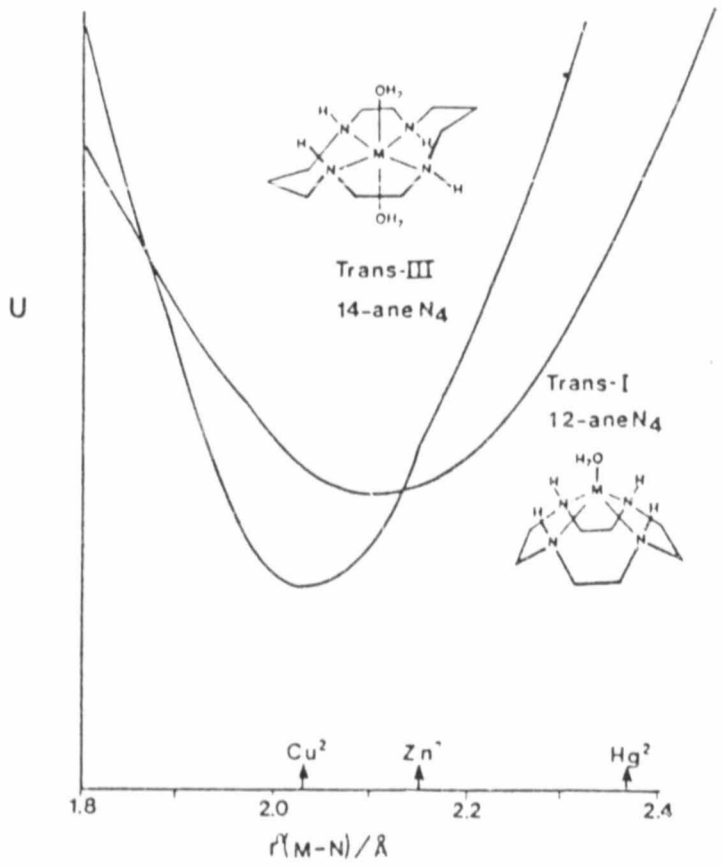


Fig. 1.4.4 Total strain energy (U) versus $r^{o}$ curve for the trans–I form of 12–ane$N_4$ and the trans–III form of 14–ane$N_4$. Redrawn after ref. 33.

The curve for the trans I conformer of 12–ane$N_4$ is flatter than that of the trans III conformer of 14–ane$N_4$ indicating that 12–ane$N_4$ should display a greater tolerance to variation in metal ion size. The minimum of this curve occurs at a larger M–N distance than that of the 14–ane$N_4$ macrocycle, implying that the best–fit size of the metal ion fitting into 12–ane$N_4$ is larger than for 14–ane$N_4$. The two conformers thus exhibit different preferences for various metal ions.

Since the trans I conformer is more stable in 12–ane$N_4$ a high stability of this

ligand with large metal ions is expected, whereas in 14–ane$N_4$ the trans III conformer is stable and therefore a decrease in stability should be observed with large metal ions (24). These findings were in good agreement with the formation constant data which later became available (Table 3). It is apparent from the data in Table 3 that the smallest metal ion $Ni^{2+}$ (S = 0) strongly prefers the larger macrocycle 14–ane$N_4$, while the large metal ion $Pb^{2+}$ strongly prefers the smaller macrocycle 12–ane$N_4$.

Table 3. Formation Constant (log $K_1$) data for 12–ane$N_4$ and 14–ane$N_4$ with a variety of metal ions.

| | $Ni^{2+}$(S=0) | $Cu^{2+}$ | $Ni^{2+}$(S=1) | $Zn^{2+}$ | $Cd^{2+}$ | $Pb^{2+}$ |
|---|---|---|---|---|---|---|
| Ionic Radius(Å)[a] | 0.45 | 0.57 | 0.69 | 0.74 | 0.95 | 1.18 |
| 12–ane$N_4$ | 13.9 | 23.29 | 16.4 | 16.2 | 14.3 | 15.9 |
| 14–ane$N_4$ | 19.9[b] | 26.5 | 19.6[b] | 15.5 | 11.23 | 10.83 |
| Δlog K | 6.0 | 3.2 | 3.2 | –0.7 | –3.1 | –5.1 |

Formation Constant data taken from reference 102.

a = reference 98. b = reference 99.

Thus, tetraazamacrocycles do not display metal–ion size–selectivity based on the match between metal ion size and the cavity in the ligand.

The association of crown ethers with alkali metal cations has been mainly described in terms of similarities between cation sizes and the size of the cavity of the crown ether (2,48). Extensive research on a series of crown ethers ranging from 12–crown–4 to 24–crown–8 has been conducted (Fig. 1.4.5).

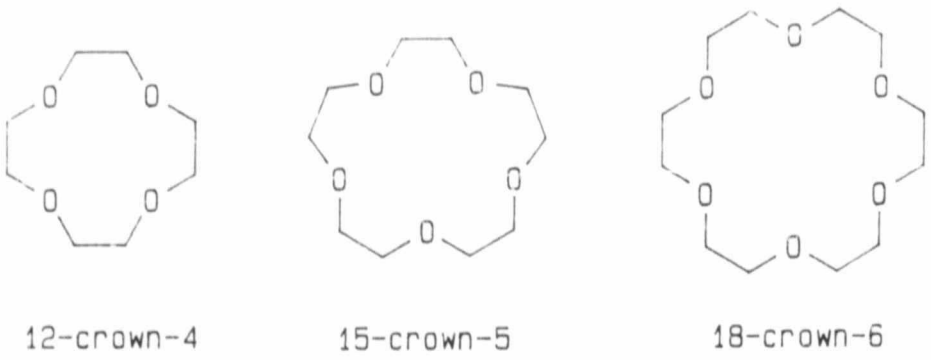


Fig. 1.4.5 Structures of some crown ethers.

With 18–crown–6 the highest stability was found for the complexes of $K^+$ and $Ba^{2+}$ which are of similar sizes and of correct sizes to fit in the cavity (49). Even the post–transition metal cations such as $Ag^+$ and $Tl^+$ followed the size–rule with 18–crown–6 which was attributed to favourable enthalpy effects (27). In the case of the smaller 15–crown–5, the smaller metal ion $Na^+$ is expected to fit best. However, this macrocycle could not accommodate the metal ion (27), and was accounted for by the high solvation energy of the $Na^+$ metal ion. Crown ethers larger than 18–crown–6 showed no metal ion size–selectivity patterns. The conclusion was that for crown ethers larger and smaller than 18–crown–6 there is no correlation between selectivity and cavity size (49).

Michaux and Reisse (28) reported thermodynamic studies on the complex formation of alkaline cations with crown ethers such as 12–crown–4, 15–crown–5 and 18–crown–6. No correlation was found between the thermodynamic parameters and the cation or crown ether sizes. Solvation of the cation was thought to play an important role (28).

Recently, equilibrium stability constant determination on a homologues series of crown ethers has been reported by Gokel et al. (29). The results are shown graphically in Fig. 1.4.6. If the widely accepted "hole–size–selectivity" rule is to be obeyed, then $Na^+$ should have the highest stability with 15–crown–5. This is not what was observed (Fig. 1.4.6), the $Na^+$ cation formed a more stable complex with the larger 18–crown–6 macrocycle. Regardless of the size of the macrocycle studied, the most stable complex formed was that with the $K^+$ cation and the most stable complexes of all the cations studied was with 18–crown–6 (29). These findings conclusively reveal that the "hole–size–selectivity" pattern is not applicable to crown ethers.

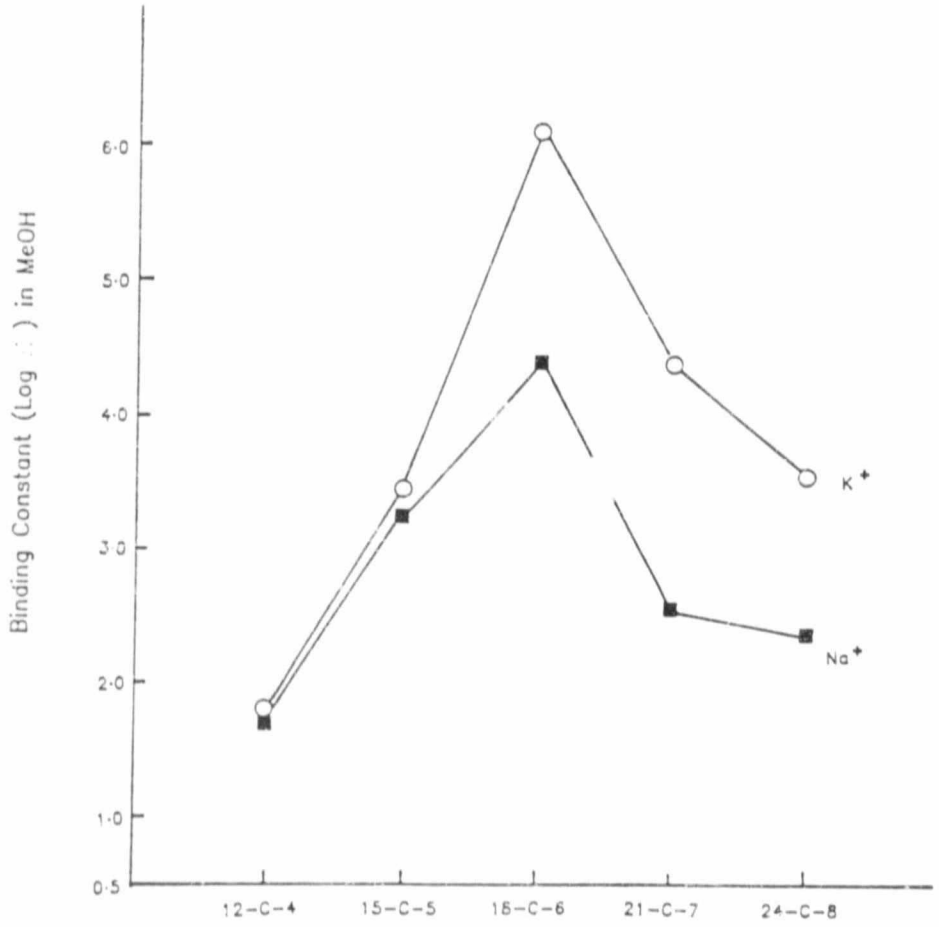


Fig. 1.4.6 Cation binding by simple crown ethers. Data taken from ref. 29.

Various crystal structures of crown–ether complexes suggest that the crown ethers are flexible and are capable of "wrapping" around the metal cation (30). Large crown–ethers are capable of twisting and so adjusting the cavity to the size of the smaller cation. This would account for large crown–ether macrocycles being able to form complexes with small cations such as the $Na^+$ cation.

Kollman et al. (31) investigated the structural flexibility of the complexed and uncomplexed 18–crown–6 using molecular mechanics calculations. For the uncomplexed crown–ether several structures of low energy were found. The different conformations were characterized by symmetry type, using the notation $D_{3d}$, $C_i$, $C_2$ and $C_1$. The relative stabilities of these structures were dependent on the electrostatic charge on the atoms and thus on the change in dielectric constant.

With a dielectric constant of unity, the $C_i$ structure of the crown was found to be the most stable. This stability was attributed to its low internal electrostatic energy. With the $K^+$–crown and $Na^+$–crown complexes, the $D_{3d}$ and $C_i$ structures respectively were found to be more stable. In the case of $Na^+$–crown the stability was due to low energy $M^+$–crown interaction whereas with $K^+$–crown the $D_{3d}$ conformation had a low internal strain energy even though the $M^+$– crown interactions were not favourable. The intrinsic interaction energy of the cations with the crown was $Na^+ > K^+ > Rb^+ > Cs^+$ and cation specificity of 18–crown–6 in solution was governed by the balance between the crown–cation interaction energies and cation solvation.

With mixed nitrogen–oxygen donor macrocycles, Hancock et al. (32) studied the stabilities of metal complexes with increase in cavity of the macrocycle with the view of investigating the "hole–size–selectivity" of metal ions. The ligands employed were 12–ane$N_3O$ and 13–ane$N_3O$. The results indicated that large metal

ions such as $Pb^{2+}$ and $Cd^{2+}$ complex more strongly with the smaller macrocycle 12-ane$N_3O$ and smaller metal ions such as $Cu^{2+}$ form more stable complexes with the larger macrocycle 13-ane$N_3O$. These results were contrary to the "hole–size–selectivity" pattern.

An obvious picture that emerges from the above discussion is that these macrocycles are too flexible to display any "hole–size–selectivity". This relationship is observed for the relatively rigid macrocycles prepared by Lehn et al. (63). With the tetraazamacrocycles, variation in cavity size is achieved by varying the size of the bridging group from ethylene to trimethylene. This would alter the size of the chelate ring formed on complex formation. An important factor in controlling complex stability in tetraazamacrocycles in thus not the size of the macrocyclic cavity, but rather the size of the chelate ring formed on complex formation. For the oxygen–donor macrocycles, variation in the size of the macrocyclic cavity is accompanied by the addition of oxygen donors plus their connecting ethylene groups. For these macrocycles it is the number of oxygen donors that governs the cation selectivity. These two factors will be discussed in sections 1.5 and 1.6 respectively.

## 1.5 THE EFFECT OF CHELATE RING SIZE

The previous discussion has indicated that factors other than simply the size of the macrocyclic cavity may be important in determining complex stability. Particularly evident was that where the size of the macrocyclic cavity is varied by varying the number of methylene groups in the macrocyclic ring, the actual factor controlling selectivity is the size of the chelate rings formed on complex formation, rather than the macrocyclic ring itself. That this is an effect of chelate ring size, rather than macrocyclic ring size, is because exactly the same type of effect is found for open–chain ligands (Fig. 1.5.1).

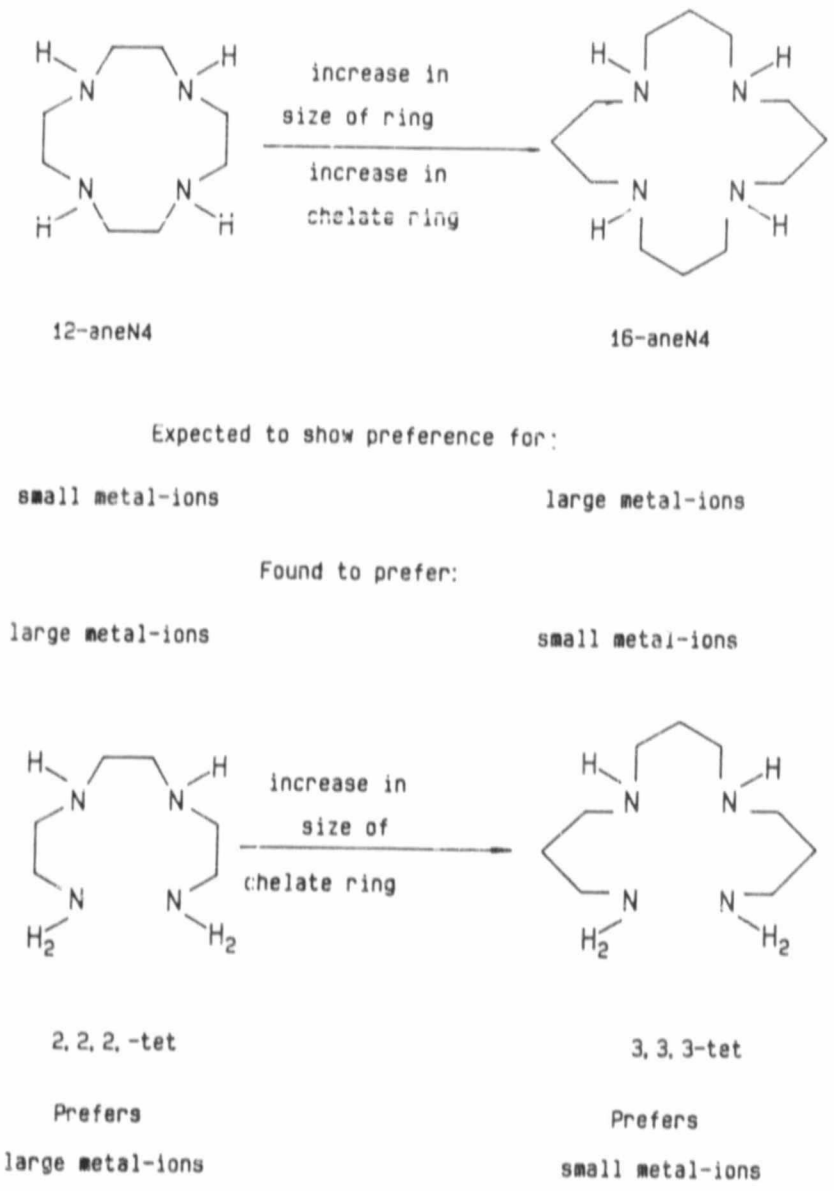


Fig. 1.5.1 The effect of the chelate ring size.

It has been shown that, if in the complex of an existing ligand, the chelate ring is increased from a five– to a six–membered ring, then the selectivity of the ligand for small metal ions will increase relative to the large metal ions (33).

The effect of the chelate ring size can firstly be demonstrated by the open chain ligands such as EDTA and TMDTA (Fig. 1.5.2). EDTA forms a five–membered chelate ring between its two nitrogens on complex formation, while TMDTA forms a six–membered chelate ring. In moving from EDTA to TMDTA there is a progressive decrease in the stabilization of large metal ions. This can be seen in Fig. 1.5.3 where the change in complex stability, $\Delta$log K, in going from EDTA to TMDTA, is plotted against ionic radius. It is seen that as the metal ion radius increases, the complex stability decreases on passing from the five–membered chelate ring to the six–membered chelate ring. Thus, EDTA has a $Pb^{2+}$ over $Zn^{2+}$ selectivity of 1.6 log units whereas that of TMDTA is –1.5 log units. The same type of selectivity pattern is observed for the tetraazamacrocycles (33). The change in complex stability for the macrocycles 12– through 16–ane$N_4$ relative to the stability of the 12–ane$N_4$ is shown in Fig. 1.5.4. It is seen that as the macrocyclic ring size is increased the complexes of the larger metal ions such as $Pb^{2+}$, $Cd^{2+}$ and $Hg^{2+}$ decrease in stability. This result is obtained even for the open chain tetraaza analogues (33). Thus, the metal ion preferences displayed by ligands forming five– and six–membered chelate rings is independent of the macrocyclic structure. By replacing a single nitrogen in the tetraazamacrocycles by an oxygen donor to form 12–ane$N_3O$ and 13–ane$N_3O$ exactly the same selectivity pattern is observed (Fig. 1.5.2) (32). This selectivity pattern is observed even with the crown ethers (Fig. 1.5.2). Crown ether II which forms two six–membered chelate rings, is known to have a higher selectivity for the small $Li^+$ ion over the larger $Na^+$ ion compared to crown ether I (68).

A large number of literature data on formation constants suggest that the chelate ring size effect is general, especially where the donor atoms in the chelate ring are nitrogen and/or oxygen. Thus, the metal–ion size–selectivity behaviour is independent of the macrocyclic structure.

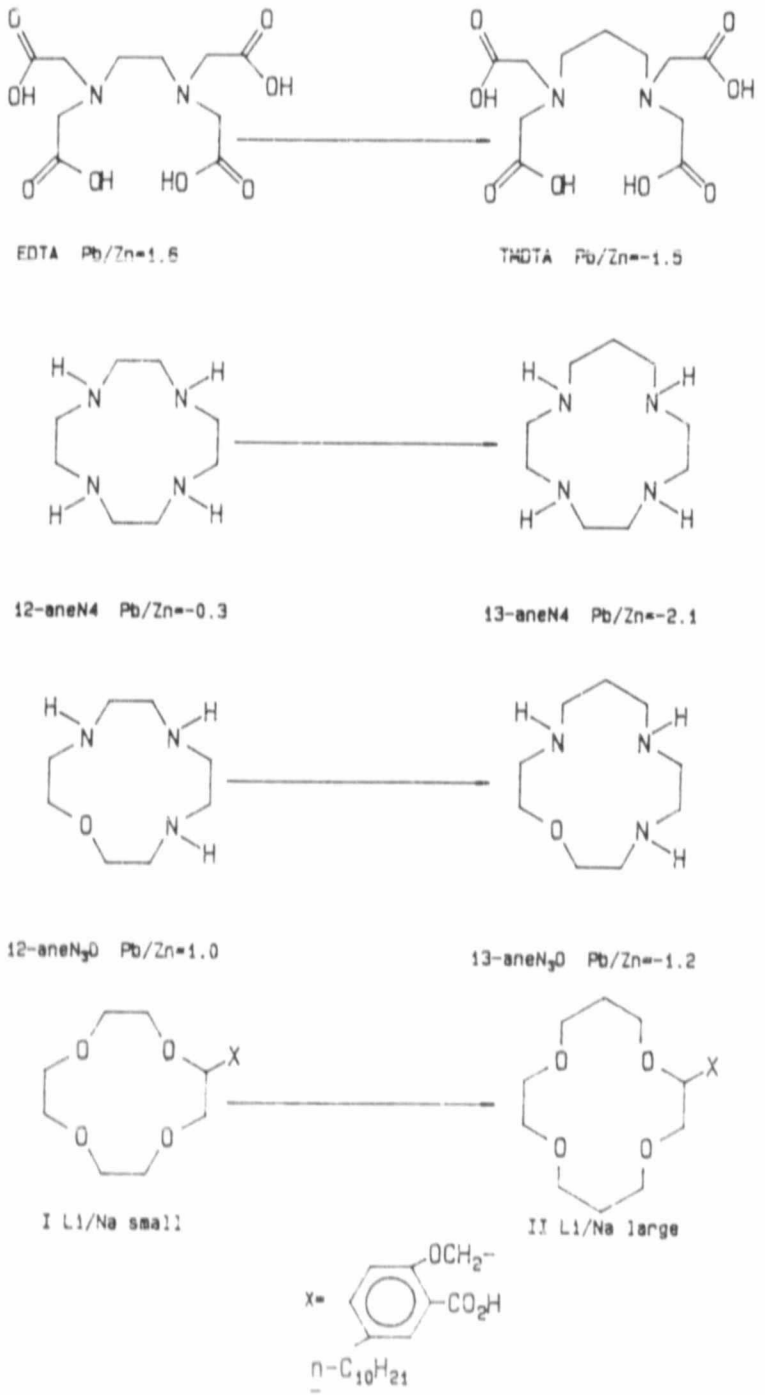


Fig. 1.5.2 Effect of chelate ring size in both open–chain and macrocyclic ligands on the $Pb^{2+}$ over $Zn^{2+}$ selectivity. The $Pb^{2+}/Zn^{2+}$ selectivity is log $K_1(Pb^{2+})$ minus log $K_1(Zn^{2+})$ for each ligand.

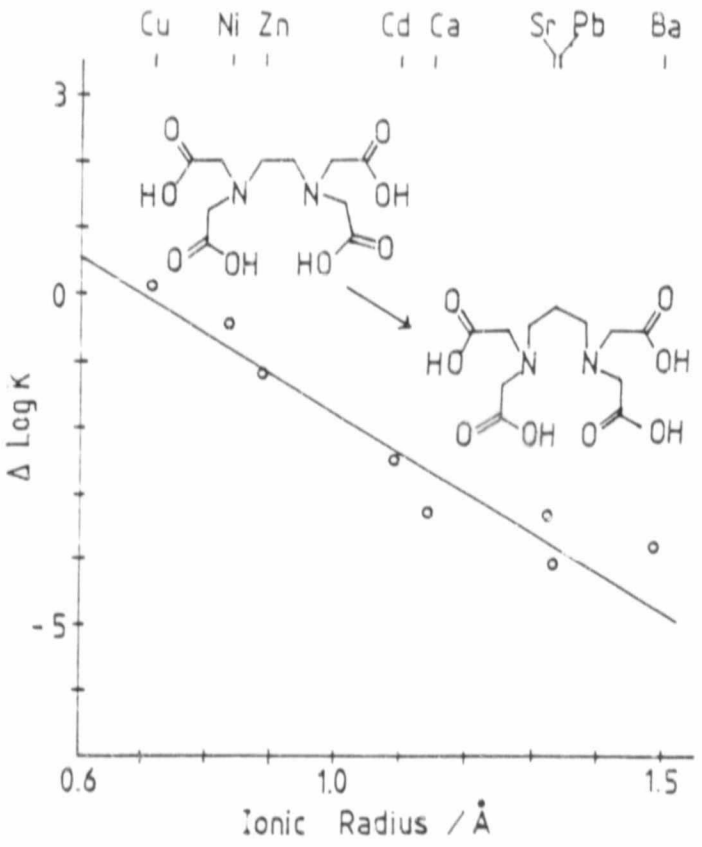


Fig. 1.5.3 Change in complex stability, Δ log K, as a function of metal ion radius as the chelate ring is increased from five– to six–membered ring. The pair of ligands where the increase is occurring are EDTA and TMDTA.

A general view was that the lower stability of the small metal–ion complexes with ligands that form six–membered rings was due to steric strain. Empirical force–field calculations have been used (69–72) to analyse the conformation of the chelate rings and differences in stability between related chelating ligands. In most cases, the strain energy calculations were performed on complexes of $Co^{3+}$ on which no thermodynamic data was available.

McDougall et al. (34) used $Ni^{2+}$ complexes of a series of polyamines (Fig. 1.5.5) to calculate the strain energies. These energies were compared to the thermodynamic parameters obtained by other workers.

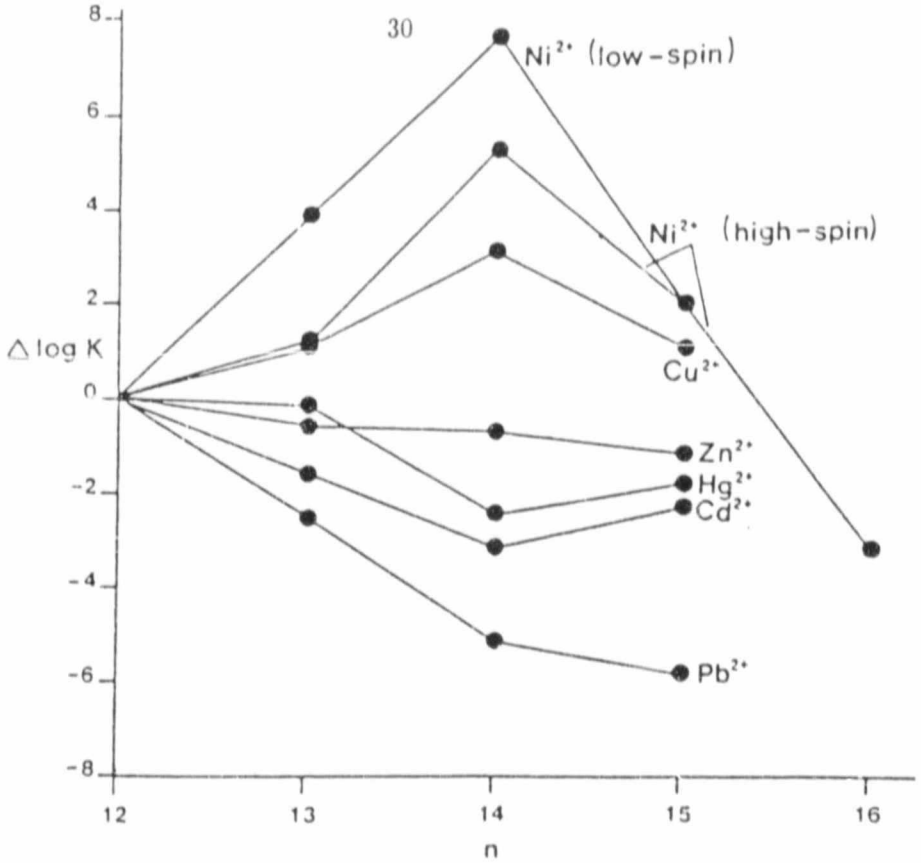


Fig. 1.5.4 Stability of complexes of n–ane$N_4$ macrocycles relative to the stabilities of the 12–ane$N_4$ complex as a function of n, the number of atoms in the macrocyclic ring of n–ane$N_4$.

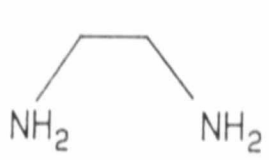


EN

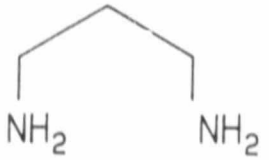


PD

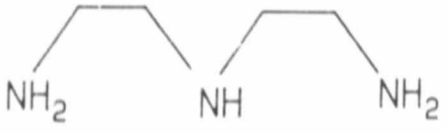


DIEN

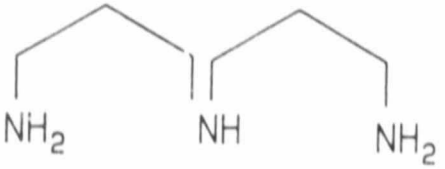


DPTN

Fig. 1.5.5 Structures of the polyamines given in Table 4.

With an increase in chelate ring size there was an increase in strain energy and a less negative enthalpy of complex formation. This is shown in Table 4. For a pair of complexes, where one member of the pair has a five–membered chelate ring and the other member of the pair has a six–membered chelate ring, the change in strain energy on complex formation, $\Delta U$, agrees well with the differences in $\Delta H$ (34).

Table 4. The difference in the total strain energies and enthalpy on complex formation on increasing the chelate ring size from five– to six–membered. Units are kcal.mol$^{-1}$.

| Complex | Total conformational energy (U)[a] | $\Delta U$[a] | Enthalpy of complex formation ($\Delta H$) | $\Delta(\Delta H)$[a] |
|---|---|---|---|---|
| $[Ni(EN)_3]^{2+}$ | 4.57 | 7.72 | −27.9[a] | 6.6 |
| $[Ni(PD)_3]^{2+}$ | 13.11 | | −21.3[a] | |
| $[Ni(DIEN)_2]^{2+}$ | 11.86 | 8.35 | −25.3[b] | 7.7 |
| $[Ni(DPTN)_2]^{2+}$ | 21.31 | | −17.6[b] | |

[a] Ref. 34

[b] Ref. 100

To understand further the effect of the chelate ring size on complex formation, Hancock et al. (35) have calculated strain energies of the chelate rings formed with EN and PD with a generalized metal ion. With the EN chelate ring, minimum strain energy was obtained for M–N bond length of 2.5Å and N–M–N angle of 69°. The minimum strain energy for the PD chelate ring was obtained for M–N bond length of 1.6Å and N–M–N angle of 109.5Å (Fig. 1.5.6). These findings are in accord with the fact that as the metal ion size increases, the L–M–L bond angle

within the chelate ring decreases, because of the increase in coordination number of the metal ion. Thus, as the M–L bond length increases the L–M–L angle decreases. Since the ligand EN, which forms a five–membered chelate ring, has minimum strain energy at large M–L bond lengths and small L–M–L angles, large metal ions are expected to coordinate more favourably.

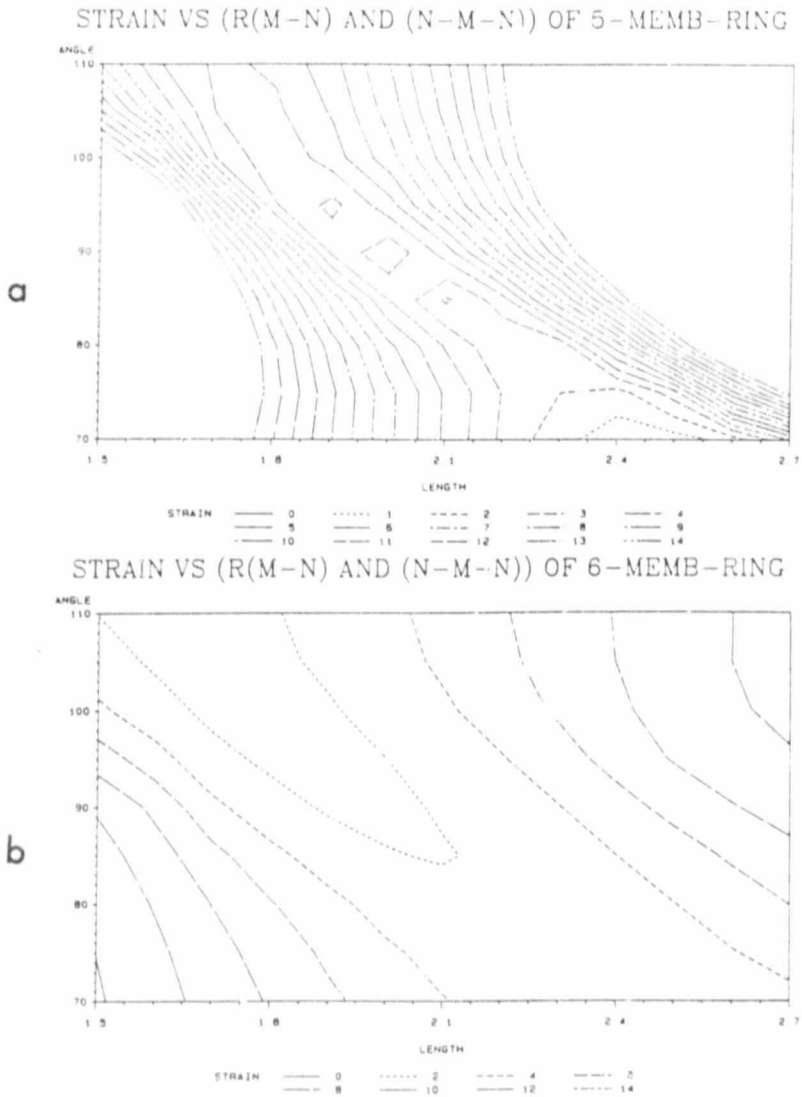


Fig. 1.5.6 Strain energy versus [(M–N distances) and (N–M–N angles)] of a) a five membered chelate ring and b) a six membered chelate ring.

The ligand PD forms a six–membered chelate ring and has minimum strain energy at small M–L bond lengths and large L–M–L angles, so that a higher affinity of this ligand with small metal ions is expected. These calculations provide a reasonably good explanation for the metal–ion stability pattern observed in ligands which form five– and six–membered chelate rings.

The chelate ring size can be further rationalized in terms of the cyclohexane ring where the lowest strain is observed for the chair conformation which has all bond angles equal to 109.5° (Fig. 1.5.7). In order for the six–membered chelate ring to achieve this conformation, the metal ion has to be of a size similar to the carbon atom and have N–M–N angles of 109.5°. The result is that large metal ions cause a deviation from the ideal tetrahedral angle of 109.5° since the angle around the nitrogen is increased. This introduces strain due to angle bending. To minimize this strain six–membered chelate rings would prefer smaller metal ions (36).

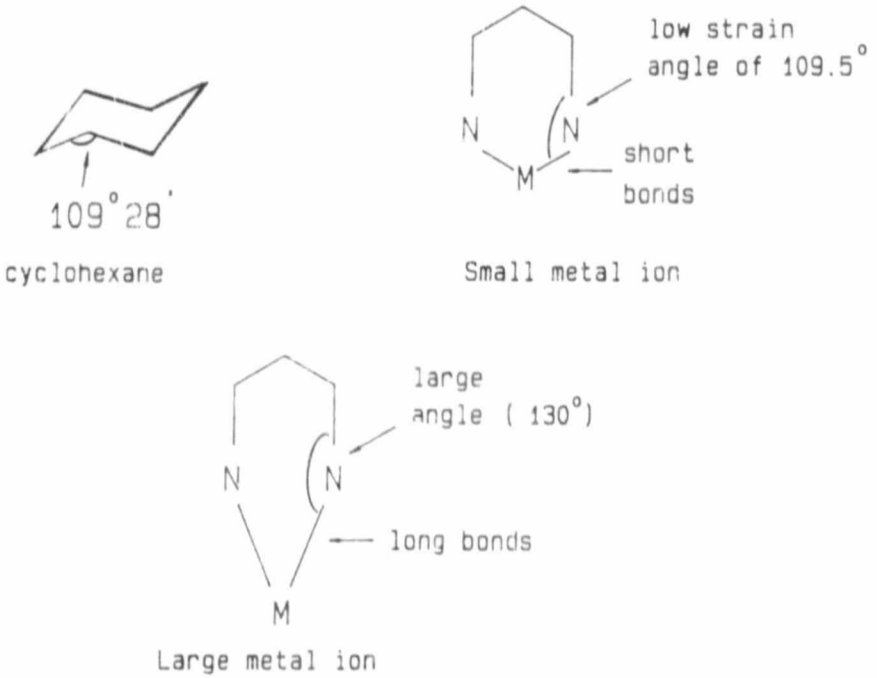


Fig. 1.5.7 The six membered chelate ring.

The ideal bite size (N–N distances across the chelate ring) for five– and six–membered chelate rings is the distance between carbon atoms 1 and 4 and carbon atoms 1 and 5 respectively (Fig. 1.5.8). The bite size of five–membered chelate rings is larger than that of six–membered chelate rings; thus six–membered chelate rings would be less strained when a small metal ion is involved.

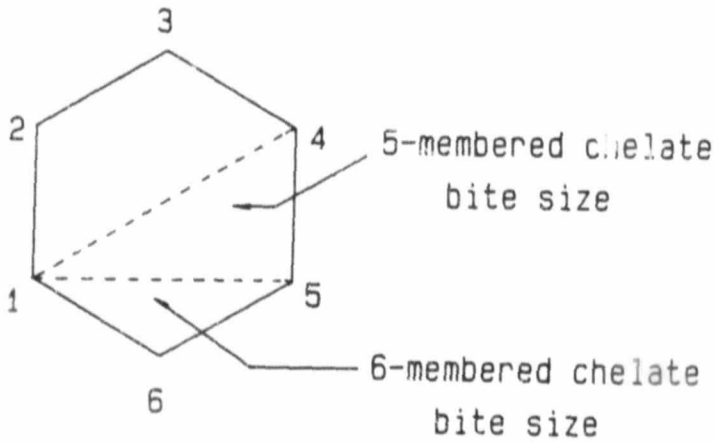


Fig. 1.5.8 The five– and six–membered chelate bite size.

Hancock et al. (37) reported that the metal–ion size–selectivity pattern in tetraazamacrocycles levels off after two five–membered chelate rings have been converted to six–membered chelate rings whereas for the open chain tetraamines the reverse size–selectivity was observed after one such change. For EDTA complexes, this size selectivity pattern was observed even after four acetate groups have been converted to proprionates. The reverse in selectivity patterns was attributed to steric crowding which produces an increased destabilization for smaller metal ions (38).

By increasing the chelate ring size to seven– and eight–membered chelate rings in tetraazamacrocycles, Hancock and Ngwenya (39) observed a uniform drop in complex stability for all the metal ions. Similar behaviour was found with the

**Author** Bhavan Rekha
**Name of thesis** Ligand Design Using The Neutral Oxygen Donor To Control Metal Ion Size Selectivity. 1989

***PUBLISHER:***

**University of the Witwatersrand, Johannesburg**
**©2013**

***LEGAL NOTICES:***

**Copyright Notice:** All materials on the University of the Witwatersrand, Johannesburg Library website are protected by South African copyright law and may not be distributed, transmitted, displayed, or otherwise published in any format, without the prior written permission of the copyright owner.

**Disclaimer and Terms of Use:** Provided that you maintain all copyright and other notices contained therein, you may download material (one machine readable copy and one print copy per page) for your personal and/or educational non-commercial use only.

The University of the Witwatersrand, Johannesburg, is not responsible for any errors or omissions and excludes any and all liability for any errors in or omissions from the information on the Library website.